

A systematic study of antibacterial silver nanoparticles: efficiency, enhanced permeability, and cytotoxic effects

Manuel I. Azócar · Laura Tamayo · Nelson Vejar · Grace Gómez ·
Xiangrong Zhou · George Thompsom · Enrique Cerda · Marcelo J. Kogan ·
Edison Salas · Maritza A. Paez

Received: 25 June 2013 / Accepted: 16 May 2014 / Published online: 15 August 2014
© Springer Science+Business Media Dordrecht 2014

Abstract We report here a systematic study of the antibacterial behavior of silver nanoparticles coated with fatty acids (oleic: AgNP-O, linoleic: AgNP-L, and palmitic acids: AgNP-P) in water. We have found remarkable differences in their capability to penetrate bacteria cell over a broader range of particle size of ~4–96 nm compared to previously reported work, and a variable toxicity depending on the particles size. Our results indicate that silver nanoparticles stabilized with oleic acid showed clear advantages in antibacterial activity, penetration inside the bacteria cells, cytotoxicity, time effectiveness, efficiency, and stability against light.

Keywords Silver · Nanoparticles · Antibacterial · Cytotoxicity · Permeability · Environmental and health effects

Introduction

Since ancient times, the silver ion has been known to be effective against a broad range of microorganisms. In the last decade, this metal has been extensively studied as nanosized metallic particles for antibacterial capability against a broad range of bacteria, viruses, and fungi (Xiu et al. 2012; Taglietti et al. 2012; Marambio-Jones and Hoek 2010; Elechiguerra et al. 2005). The scientific community has focused a great amount of effort to understand the antibacterial activity of silver, but the scientific debate concerning

Electronic supplementary material The online version of this article (doi:10.1007/s11051-014-2465-4) contains supplementary material, which is available to authorized users.

M. I. Azócar (✉) · L. Tamayo · N. Vejar ·
G. Gómez · E. Salas · M. A. Paez
Facultad de Química y Biología, Universidad de Santiago
de Chile, Avenida Bernardo O'Higgins 3363, Casilla 40,
Correo 33, Santiago, Chile
e-mail: manuel.azocar@usach.cl

M. A. Paez
e-mail: maritza.paez@usach.cl

X. Zhou · G. Thompsom
Corrosion and Protection Centre, School of Materials, The
University of Manchester, Manchester M13 9PL,
England, UK

E. Cerda
Departamento de Física, Facultad de Ciencias,
Universidad de Santiago de Santiago de Chile,
Avenida Ecuador 3493, Santiago, Chile

M. J. Kogan · E. Salas
Facultad de Ciencias Químicas y Farmacéuticas,
Universidad de Chile, Calle Sergio
LivingstonePolhammer 1007, Santiago, Chile

the mechanism still continues. Some authors have suggested that the antibacterial capability relies on silver ions released from bulk metallic silver or from the surfaces of nanoparticles, followed by the interaction of Ag^+ ions with thiol groups in bacterial proteins or by interfering with DNA replication (Marambio-Jones and Hoek 2010; Feng et al. 2000; Wu et al. 2009; Cioffi and Rai 2012). It has also been reported that silver ions interact with the cell wall, causing cell lysis (Cioffi and Rai 2012).

From this perspective, silver nanoparticles have been reported to be more active over time than an equivalent mass of silver ions (Kong and Jang 2008). Such behavior has been considered to be related to the high surface/volume ratio typically present in nanomaterials, i.e., for smaller particles with a large metallic surface it is favored a higher biocidal effect (Morones et al. 2005). Regarding the mechanism which explains their high antibacterial activity, investigations have found that it relates primarily to the release of silver ions from the surface of the nanoparticles (Xiu et al. 2012; 2011). However, Xu et al., studying the membrane transport mechanism of living microbial cells (*Pseudomonas aeruginosa*) using chloramphenicol to increase membrane permeability, demonstrated that Ag nanoparticles (AgNPs) with sizes ranging up to 80 nm are accumulated in living microbial cells (Xu et al. 2004).

Further, several studies have focused on the cytotoxic effects of AgNPs with preliminary conclusions partially attributed to the release of silver ions. Consequently, an inverted relationship between toxicity and nanoparticle size is suggested, and associated with the typical high surface/volume ratio present in nanomaterials (Xiu et al. 2011). Regardless of the cytotoxic mechanism, increased commercial application of AgNPs may have negative impact on human health and the environment (Lowry et al. 2012). Therefore, it is necessary to use the lowest possible doses with minimal cytotoxic effects.

In this study, we found a remarkable effect of oleic acid as coating on the permeability of AgNPs through the cell membrane, antibacterial effectiveness, stability over time, and cytotoxic effects in comparison with other fatty acid and bare nanoparticles in a diameter of ~4–100 nm.

Experimental procedure

Synthesis and characterization of AgNPs

Silver nanoparticles were synthesized using the previously reported method (Wang et al. 1999, 1998). The size of the AgNPs was controlled using 5.0×10^{-4} (sample 1), 9.0×10^{-4} (sample 2), 1.3×10^{-3} (sample 3), 1.7×10^{-3} (sample 4), 2.1×10^{-3} (sample 5), and 2.5×10^{-3} M (sample 6) of AgNO_3 . Spherical silver nanoparticles (AgNps) were prepared by chemical reduction of silver nitrate solution (samples 1–6) in presence and absence of fatty acids (3.0×10^{-3} M) as a coating, mixed with fresh sodium borohydride (3.0×10^{-2} M) at 20 °C and vigorous stirring. A brown colloidal solution stabilized by fatty acid is obtained and stored in amber bottles to protect from light.

Samples of fresh nanoparticles were centrifuged, washed, and dispersed in water. The concentration of metal in the aqueous medium was measured by dissolution in HNO_3 and Inductively Coupled Plasma (ICP) prior to antibacterial experiments.

The morphology and size of silver nanoparticles were examined in a FEI-Tecnaï F20 Transmission electron microscope (TEM). Additionally, the size of AgNps was estimated with a dynamic light scattering (DLS) instrument (Malvern Instruments, Zetasizer Nano S-90).

Antimicrobial Activity (MICs)

Antimicrobial activities of complexes were determined according to the recommendations of NCCLS (1999), National Committee for Clinical Laboratory Standards, by the use of a broth microdilution method. Minimum inhibitory concentrations (MICs) for the tested AgNPs were prepared in presence of *Escherichia coli* (ATCC 25922). Silver nanoparticles stock solutions were diluted in broth solution to the final concentrations of 5, 10, 15, 20, 25, 30, 35, 40, 45, and 50 $\mu\text{g}/\text{mL}$. MIC determinations were performed in Muller Hinton Broth and registered after 24 h incubation at 37 °C of 10^5 CFU/mL in the respective AgNps concentrations. The inocula were prepared from a 10^6 CFU/mL starting inoculum grown at 37 °C overnight. The MIC value corresponded to the lowest concentration that inhibited the bacterial growth.

Antibacterial effectiveness over time

Solutions of the samples 2 (small), 4 (medium), and 6 (large) of AgNps (10 µg/mL) were used in a culture of 10^5 , 10^4 , 10^3 , 10^2 , and 10^1 CFU/mL of *E. coli*. Samples of 300 µL was transferred (in sextuple) in 96 well immunoplates (ELISA Plates) and incubated for 24 h at 37 °C under shaking condition (in Muller Hinton Broth). The growth inhibiting effect was measured using optical density at 629 nm (Labsystem Miltiskan, 352 and Ascent v. 2.6 Software) as a function of time under the presence of AgNps (AgNP, AgNP-O, AgNP-L, and AgNP-P) and recorded every 1 h up to 24 h.

Transmission electron microscopy for AgNPs inside the *E. coli* cells

An aliquot of 3 mL of bacteria solution, standardized to 10^5 CFU/mL, was and incubated for 45 min in presence of AgNPs. After the incubation period, the samples were washed with buffer and centrifuged at 3000 rpm for 12 min to obtain a pellet of bacteria. The pellet was fixed by exposure to a 2.5 % glutaraldehyde solution in cacodylate buffer for 30 min followed by a dehydration of the bacteria using 50, 60, 70, 90, and 100 % ethanol/cacodylate buffer solutions. The bacteria were finally embedded into epoxy resin and left to polymerize in an oven at 60 °C for 24 h. The samples were sectioned in slices of thickness of 100 nm and deposited in copper grid (400 mesh) and observed in TEM Philips Tecnai 12 (Tamayo et al. 2014).

Cell viability assays by confocal microscopy

Bacteria samples of 10^4 CFU/mL were tested for a dose of 10 µg/mL and cultured in sterile Muller Hinton Broth at 37 °C. Samples were taken every 30, 60, 90, 120, and 160 min, centrifuged and subsequently the samples were stained with live/dead[®] (marked green for live bacteria, and dead bacteria in red) and allowed to stand for 15 min. The samples were washed with 0.85 wt% NaCl solution to remove excess stain. Finally, the samples were deposited on the slide and covered with coverslip and sealed with tape to be observed in the confocal microscope Carl Zeiss LSM 700. Photographs were obtained with a digital camera (Olympus, 3.2 Mpix). The ratio of

green to red fluorescent cells provides a quantitative index of bacterial viability (Chamakuraa et al. 2011).

Stability methodology

UV–Vis absorbance spectra of the AgNPs in solution were recorded at different times (1, 5, and 12 days) in order to observe intensity changes at plasmon band on a Shimadzu UV-1800 UV–Vis spectrophotometer. The average diameter of the AgNPs at the same times was estimated with a dynamic light scattering (DLS) instrument (Malvern Instruments, Zetasizer Nano S-90) in order to study agglomeration effects of the nanoparticles samples.

Cell viability Assay by MTT

In order to determine the effect of the different fatty acid-coated AgNPs on cell viability (AgNP-O, AgNP-L, AgNP-P, and AgNP-bare), a tetrazolium salt reduction assay (CellTiter 96[®]) was performed, which allowed the establishment of a linear relationship between the viable cell number and absorbance. For this assay, SH-SY5Y cells were seeded using dulbecco's modified eagle's medium (DMEM) without red phenol, on 96 well plates at a density of 6,000 cell/well. Cells were then treated with three different ratios of AgNPs at same concentration, coated with oleic, linoleic, and palmitic acid. After 24 h of incubation at 37 °C, 5 % CO₂, cells viability were measured (in triplicate). The absorbance was read at 490 nm on a Multiscan reader. The statistical analysis of data was made with Kruskal–Wallis test with a criterion for statistical significance of $p < 0.05$, using the GraphPad Prism 5.03 program (GraphPad software, Inc.).

Results and discussion

We started by synthesizing four different types of silver nanoparticles, stabilized with oleic acid, linoleic acid, and palmitic acid, respectively, and bare nanoparticles dispersed in water with particle sizes in the range of ~4–100 nm (Table 1 and S1 in supporting information). The antibacterial properties were tested against *E. coli*, as illustrated in Fig. 1b. Bare AgNPs are slightly large in size, but the size distribution of AgNPs stabilized with fatty acid is in the range of 3–90 nm and highly reproducible in every case.

Table 1 Size distribution of silver nanoparticle of six different samples, prepared from different AgNO₃ concentrations

Sample no.	Size (nm)			
	AgNP	AgNP-O	AgNP-P	AgNP-L
1	12 ± 8	6 ± 4	13 ± 4	6 ± 5
2	18 ± 13	12 ± 5	20 ± 6	12 ± 6
3	19 ± 11	17 ± 4	28 ± 12	15 ± 6
4	37 ± 17	21 ± 9	34 ± 13	22 ± 8
5	45 ± 16	34 ± 7	40 ± 11	35 ± 8
6	66 ± 19	42 ± 19	46 ± 8	43 ± 20

Plots include the size distribution obtained from DLS

AgNP Ag nanoparticles without fatty acid, AgNP-O Ag nanoparticles stabilized with oleic acid, AgNP-P Ag nanoparticles stabilized with palmitic acid, AgNP-L Ag nanoparticles stabilized with linoleic acid

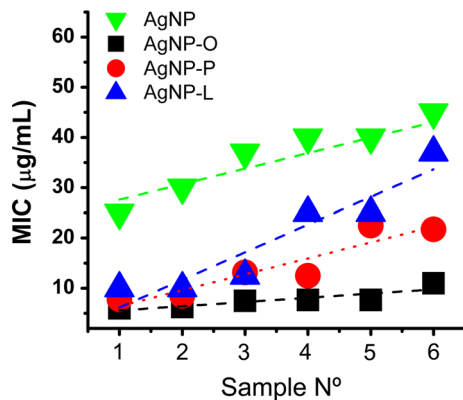


Fig. 1 Minimum inhibitory concentration values of antibacterial activity in function of the particle size and the fatty acid. AgNP: Ag nanoparticles without fatty acid, AgNP-O: Ag nanoparticles stabilized with oleic acid, AgNP-P: Ag nanoparticles stabilized with palmitic acid, AgNP-L: Ag nanoparticles stabilized with linoleic acid

When evaluating similar particle size, AgNP-O showed a remarkable antibacterial activity (Fig. 1) compared to other AgNPs. The antibacterial activity of AgNP-O is almost independent of particle size with a dose of 5–10 µg/ml against *E. coli*. AgNP-P, AgNP-L, and bare nanoparticles show similar behavior to that reported by other authors where the antibacterial activity is size dependent (Morones et al. 2005).

In order to assess the antibacterial effectiveness over time, time-killing curves were performed for 12 days in a range of 1×10^1 and 1×10^5 CFU/mL. The results in Fig. 2 show the maximum antibacterial

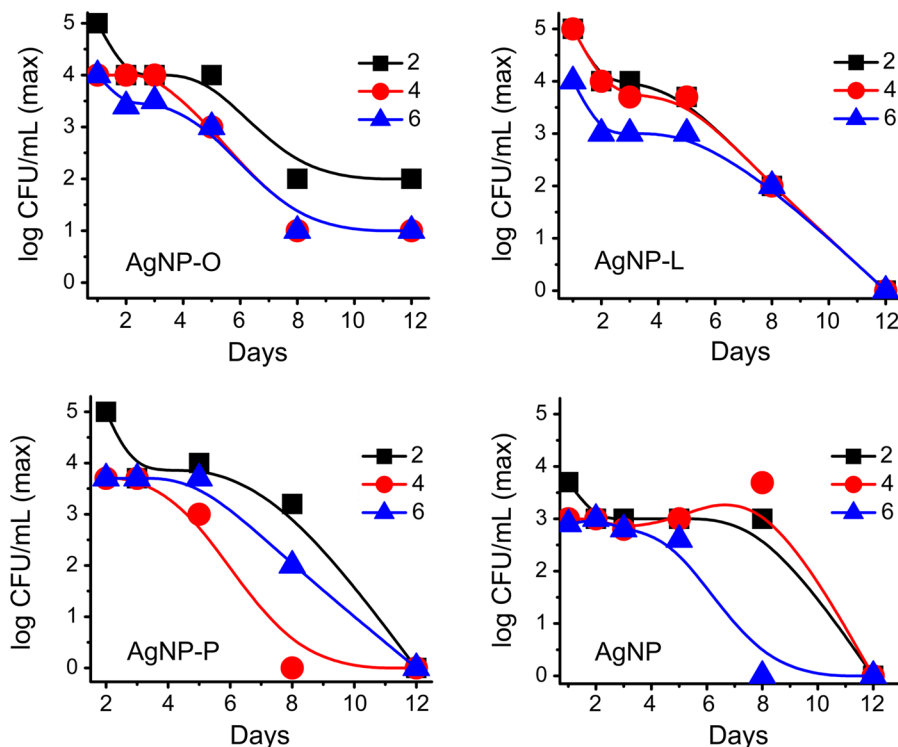
activity of the differently functionalized AgNPs over time with a dose of 10 µg/ml. Bare AgNP shows a reduced antibacterial effect, causing maximum antibacterial effect of 1×10^4 CFU/mL, even with fresh samples and using small size particles (2–30 nm). In contrast, the AgNPs stabilized with fatty acids reveal an improvement of the antibacterial behavior with the smallest nanoparticles (2–30 nm), causing lysis of 1×10^5 CFU/mL in the first day. However, nanoparticles stabilized with oleic acid (AgNP-O) showed a noteworthy antibacterial activity even after 12 days. The smaller loss of activity over time revealed by the AgNP-O, compared with AgNP-L and AgNP-P, could be determinant for its selection as an antimicrobial agent with a lowest possible doses and maximum activities over time.

Regarding the role of fatty acids in the permeability (Zhang and Rock 2008) of the *E. coli* cell wall, the transmission electron microscopy (TEM) images of Fig. 3 are revealing that the mentioned acids increase the cell penetration. From these results, the nanoparticles functionalized with oleic acid (AgNP-O) successfully penetrate the microbial cell wall, in sizes up to 96 nm. This nanoparticle size value is six times higher than those reported in other studies (Morones et al. 2005). In contrast, the bare silver nanoparticles (AgNP) show no penetration throughout the size range studied, displaying a large amount of agglomerated AgNP outside the cell wall. In the case of silver nanoparticles stabilized with palmitic and linoleic acids, with sizes between 6 and 45 nm in diameter, they are displayed within and outside the cell wall and, in several cases agglomerated.

From the above information, it is clear that the selection of the stabilizer for the nanoparticle is a key to obtain the best ratio (bactericidal efficiency/nanoparticle size) and to minimize the negative impact of the AgNPs. Therefore, a synergistic effect between both bactericidal and permeability properties (Zhang and Rock 2008) conferred by the stabilizer must be considered. Further, viability tests were conducted to correlate the permeability through the cell wall and its action over time as an antibacterial agent (see Table 2).

The kinetics of bacterial lysis for the different types of silver nanoparticles reveal different antibacterial efficiencies. The cell viability reached 0 % after 2 h of exposure to the nanoparticles stabilized with fatty acids. In contrast, the nanoparticles without any fatty

Fig. 2 Maximum antibacterial efficiency in time. Curves for small (sample 2: 2–30 nm), medium (sample 4: 8–55 nm), and large (sample 6: 25–90 nm) nanoparticles



acids were less effective, showing that, even after 160 min of exposure, the surviving populations were still in the range of 10–35 %. Therefore, AgNPs coated with fatty acids showed fast and efficient antibacterial properties compared to the uncoated AgNPs.

In order to find a correlation between the antibacterial properties of different types of nanoparticles, and the differences in loss of activity thereof with time, we studied the possible agglomeration of the AgNP by DLS measurements (Fig. 4), determining also their optical properties by UV–Vis. Figure 5 shows the absorbance values at 400 nm obtained in a period of 12 days. The selected wavelength corresponds to the maximum of the plasmon band for silver nanoparticles. For the unfunctionalized AgNP, the band intensity decreases markedly over time. In contrast, for the functionalized nanoparticles, such a decrease in intensity is clearly lower, showing a dependence on the type of fatty acid and the size of the nanoparticles. Moreover, and worthy of consideration, was the behavior of nanoparticles functionalized with oleic acid which, regardless of size, exhibit a greater stability in time. The differences observed between the

silver nanoparticles, unfunctionalized and functionalized, give evidence of the rapid oxidation of the former (Lok et al. 2007, Henglein 1998).

DLS experiments showed no significant aggregation of nanoparticles in the stock solutions, even after 12 days. However, it is clear that the presence of bacteria, and the culture broth, promote aggregation of nanoparticles (Fig. 3), which depends on the type of fatty acid used as a modifier. Thus, the role of the electrolyte is evident, particularly associated with the presence of NaCl, NaNO₃, and CaCl₂ in the culture media (Li et al. 2010, 2012), and it is here where the type of nanoparticle stabilizer plays a determining role in inhibiting coagulation of nanoparticles and consequently, their aggregation.

Going back to the main point of this study, the generation of aggregated silver nanoparticles is one of the important factors in the reduction of its antibacterial properties (Kvitek et al. 2008). Thus, selecting the optimal stabilizer of the nanoparticles becomes crucial for use in antibacterial applications.

In consideration for possible biomedical applications of AgNPs, we evaluated the toxic effect of AgNPs in neuroblastoma SH-SY5Y cell line with a

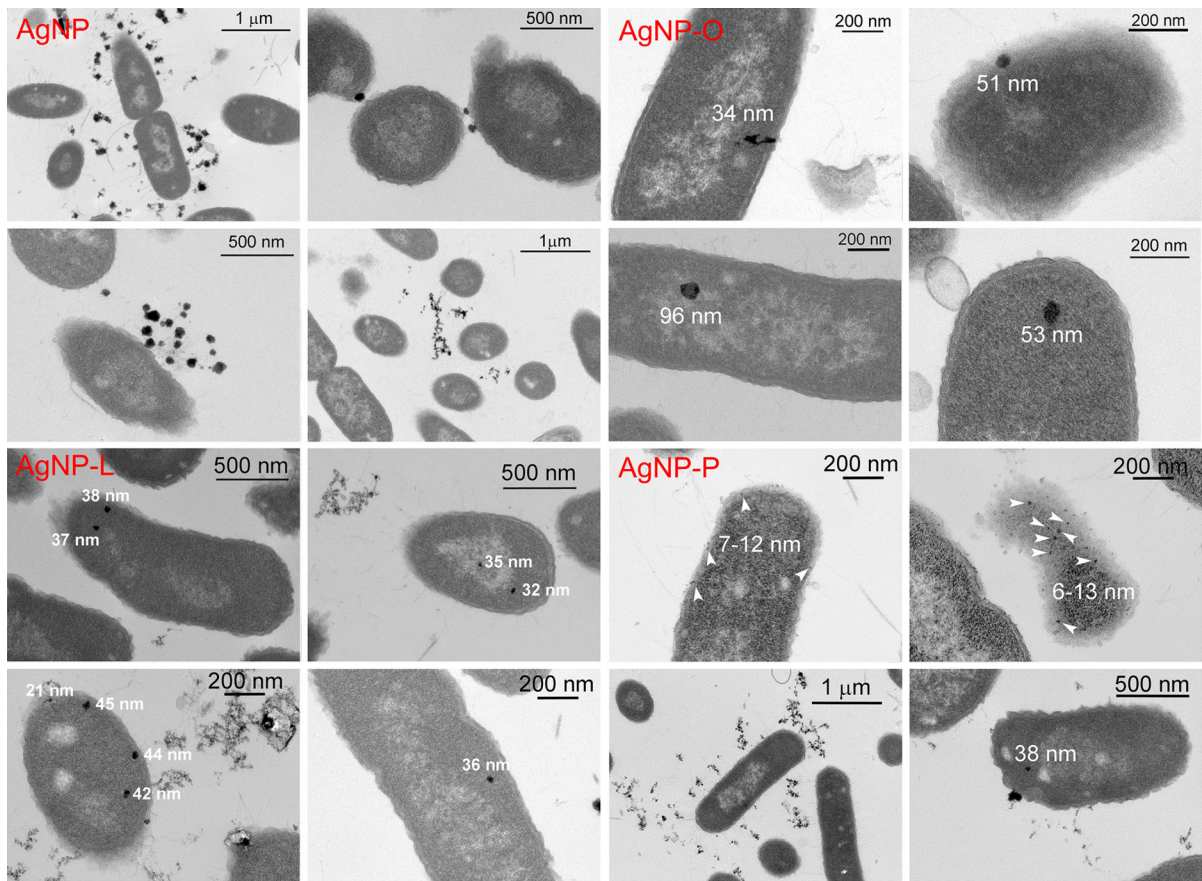


Fig. 3 TEM images show size and location of Ag nanoparticles inside the *E. coli* cells

Table 2 Viability experiments for a dose of 10 µg/ml of fresh silver nanoparticles with different sizes of 5–35 nm

	% Viability/ <i>t</i> (min)				
	30	60	90	120	160
AgNP	50–80	30–65	20–45	20–45	10–35
AgNP-O	70–75	30–50	10–40	0–20	0
AgNP-L	85–75	35–45	40–20	0–25	0
AgNP-P	80–70	50–30	30–20	0–15	0

cell proliferation assay that use mitochondrial activity of metabolically active cells as a linear indicator of cell viability. This study allowed us to obtain an approach to the *in vitro* effects of AgNPs stabilized with fatty acids. Only smaller nanoparticles show toxic effects for the neuroblastoma cells, independently of coating fatty acid, which is a size-dependent behavior (Fig. 6). Bare silver nanoparticles were not

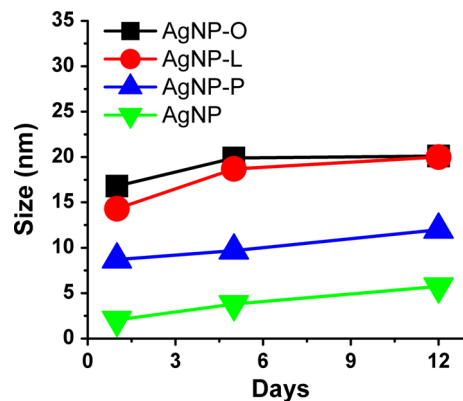


Fig. 4 Size effect based on DLS of AgNPs in water

toxic, in accordance with a stable oxidized surface, or from the presence of common ligands that can hinder the bioavailability of silver ions (Xiu et al. 2011).

In good agreement with Xiu et al. (2011), toxicity is produced and promoted by the release of Ag⁺ in the

Fig. 5 It shows the experiment over a period of 12 days. A significant decrease of the intensity in the maximum absorbance (ca. 400 nm) was observed in the bare NPs in contrast with the high stability of the UV-Visible with AgNP-O in all sizes

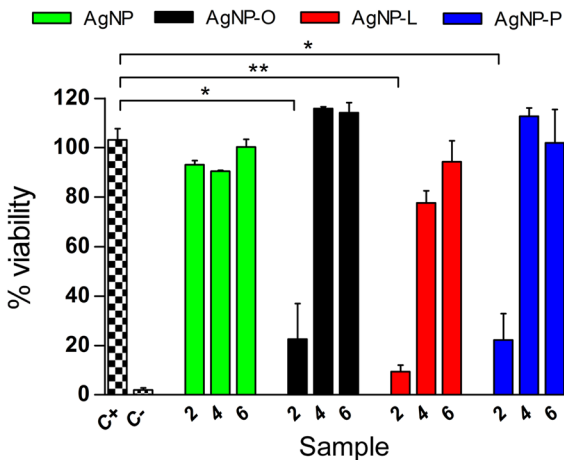
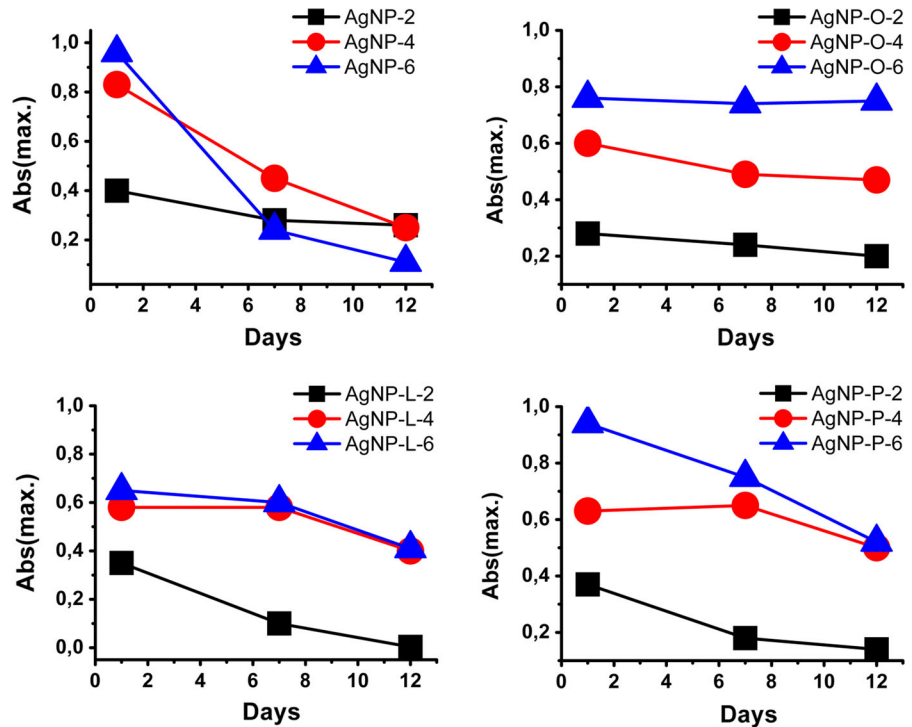


Fig. 6 Effects on cellular viability in neuroblastoma SH-SY5Y cells against samples 2, 4 and 6 (small (sample 2: 2–30 nm), medium (sample 4: 8–55 nm) and large (sample 6: 25–90 nm). C+: Positive control, C-: Negative control. Treatment at 24 h, n = 3, *p < 0.05; **p < 0.01, error bars SEM

presence of oxygen and enhanced by size effect because smaller particles release much more Ag⁺ ions than bigger, due to an increased volume/superficial area ratio. This emphasizes the importance of the size (>10 nm), rather than surface coating or functionalization in order to reduce cytotoxic effects, although

the importance of using a larger particle size, but without diminishing the antibacterial ability, which is a key factor to choose a good antimicrobial agent.

The lower toxicity of bigger coated AgNPs could be related to a slow and sustained release of ions with time (Zapata et al. 2011) and in some cases with the coating used (Beer et al. 2012; Suresh et al. 2012). Such behavior may be associated with the manner in which fatty acid molecules are rearranged around the nanoparticle and, more importantly, the strong interaction between the fatty acid units, resulting in an excellent control-barrier to the egress of silver ions (Zapata et al. 2011) allowing for one hand an efficient antibacterial effect and by other hand generating the least damage on cells, being an important issue to be addressed in future studies.

Interestingly, in this study we found that AgNPs stabilized with oleic acid showed strong advantages in antibacterial activity, time effectiveness, penetration, stability, and less cytotoxic effect.

Conclusion

In summary, we have disclosed some key findings which aid the understanding and improvement of

silver nanoparticles antibacterial efficacy in water using fatty acids as coating agents. The use of suitable stabilizers for the nanoparticles, altering the permeability of microbial cell walls, increases the possibility of penetration of the AgNP, thereby contributing significantly to improve the efficiency and effectiveness of the antibacterial ability of the nanoparticle, and most importantly, to markedly reduce AgNP the dosage to be employed and their cytotoxic effects.

While most of the work related to the antibacterial effect of silver nanoparticles, associate with silver ion release, here it is clear that the nanoparticles penetrate the microbial cell wall and, therefore, the bacteriolytic mechanism should also be considered.

Acknowledgments This work was supported by FONDECYT (Grants Nos. 1100537, and 11080133), and PIA (ACT 95). M.A. Páez and M. I. Azócar are also grateful to CONICYT (Grant 79090024). The authors also wish to thank the UK Engineering and Physical Sciences Research Council for support of the LATEST2 Programme Grant, with the characterization facilities being used in this study. We thank Dr. Carolina Perez for helpful discussion and their kind assistance.

References

- Bier C, Foldjerg R, Hayashi Y, Sutherland D, Autrup H (2012) Toxicity of silver nanoparticles: nanoparticle or silver ion? *Toxicol Lett* 208:286. doi:[10.1016/j.toxlet.2011.11.002](https://doi.org/10.1016/j.toxlet.2011.11.002)
- Chamakuraa K, Perez-Ballesteroa R, Luob Z, Bashirc S, Liu (2011) Comparison of Silver Nanoparticles Against Common Chemical Disinfectants. *J Colloids Surf B: bio-interfaces* 84(1):88–96. doi:[10.1016/j.colsurfb.2010.12.020](https://doi.org/10.1016/j.colsurfb.2010.12.020)
- Cioffi N, Rai M (eds) (2012) *Nano-antimicrobials, progress and prospects*. Springer, Heidelberg
- Elechiguerra J, Burt J, Morones J, Camacho-Bragado A, Gao X, Lara H, Yacaman M (2005) Interaction of silver nanoparticles with HIV-1. *J Nanobiotechnol* 3:6. doi:[10.1186/1477-3155-3-6](https://doi.org/10.1186/1477-3155-3-6)
- Feng QL, Wu J, Chen GQ, Cui FZ, Kim TN, Kim JO (2000) A mechanistic study of the antibacterial effect of silver ions on *Escherichia coli* and *Staphylococcus aureus*. *J Biomed Mater Res* 52(4):662–668. doi:[10.1002/1097-4636\(20001215\)52:4<662::AID-JBM10>3.0.CO;2-31](https://doi.org/10.1002/1097-4636(20001215)52:4<662::AID-JBM10>3.0.CO;2-31)
- Henglein A (1998) Colloidal silver nanoparticles: photochemical preparation and interaction with O₂, CCl₄, and some metal ions. *Chem Mater* 10:444–450
- Kong H, Jang J (2008) Antibacterial properties of novel poly(methyl methacrylate) nanofiber containing silver nanoparticles. *Langmuir* 24(5):2051–2056. doi:[10.1021/la703085e](https://doi.org/10.1021/la703085e)
- Kvitek L, Panacek A, Soukupova J, Kolar M, Vecerova R, Prucek R, Holecova M, Zboril R (2008) Effect of surfactants and polymers on stability and antibacterial activity of silver nanoparticles (NPs). *J Phys Chem C* 112(15):5825–5834. doi:[10.1021/jp7111616v](https://doi.org/10.1021/jp7111616v)
- Li XA, Lenhart JJ, Walker H (2010) Dissolution-accompanied aggregation kinetics of silver nanoparticles. *Langmuir* 26(22):16690–16698. doi:[10.1021/la101768n](https://doi.org/10.1021/la101768n)
- Li XA, Lenhart JJ, Walker HW (2012) Aggregation kinetics and dissolution of coated silver nanoparticles. *Langmuir* 28(2):1095–1104. doi:[10.1021/la202328n](https://doi.org/10.1021/la202328n)
- Lok CN, Ho CM, Chen R, He QY, Yu WY, Sun H, Tam PKH, Chiu JF, Che CM (2007) Silver nanoparticles: partial oxidation and antibacterial activities. *J Biol Inorg Chem* 12(4):527–534
- Lowry G, Gregory K, Apte S, Lead J (2012) Transformations of nanomaterials in the environment. *Environ Sci Technol* 46:6893–6899. doi:[10.1021/es300839e](https://doi.org/10.1021/es300839e)
- Marambio-Jones C, Hoek EMV (2010) A review of the antibacterial effects of silver nanomaterials and potential implications for human health and the environment. *J Nanopart Res* 12(5):1531–1551. doi:[10.1007/s11051-010-9900-y](https://doi.org/10.1007/s11051-010-9900-y)
- Morones JR, Elechiguerra JL, Camacho A, Holt K, Kouri JB, Ramirez JT, Yacaman MJ (2005) The bactericidal effect of silver nanoparticles. *Nanotechnology* 16(10):2346–2353. doi:[10.1088/0957-4484/16/10/059](https://doi.org/10.1088/0957-4484/16/10/059)
- Suresh A, Pelletier D, Wang W, Morrell-Falvey J, Gu B, Dokytycz M (2012) Cytotoxicity induced by engineered silver nanocrystallites is dependent on surface coatings and cell types. *Langmuir* 28(5):2727–2735. doi:[10.1021/la2042058](https://doi.org/10.1021/la2042058)
- Taglietti A, Diaz-Fernandez YA, Amato E, Cucca L, Dacarro G, Grisoli P, Necchi V, Pallavicini P, Pasotti L, Patrini M (2012) Antibacterial activity of glutathione-coated silver nanoparticles against gram positive and gram negative bacteria. *Langmuir* 28(21):8140–8148. doi:[10.1021/la3003838](https://doi.org/10.1021/la3003838)
- Tamayo LA, Zapata PA, Vejar ND, Azócar MI, Gulppi MA, Zhou X, Thompson GE, Rabagliati FM, Páez MA (2014) Release of silver and copper nanoparticles from polyethylene nanocomposites and their penetration into *Listeria monocytogenes*. *Mat Sci Eng C* 40:24–31. doi:[10.1016/j.msec.2014.03.037](https://doi.org/10.1016/j.msec.2014.03.037)
- Wang W, Efrima S, Regev O (1998) Directing oleate stabilized nanosized silver colloids into organic phases. *Langmuir* 14(3):602–610. doi:[10.1021/la9710177](https://doi.org/10.1021/la9710177)
- Wang W, Chen X, Efrima S (1999) Silver nanoparticles capped by long-chain unsaturated carboxylates. *J Phys Chem B* 103(34):7238–7246. doi:[10.1021/jp991101q](https://doi.org/10.1021/jp991101q)
- Wu J, Hou SY, Ren DC, Mather PT (2009) Antimicrobial properties of nanostructured hydrogel webs containing silver. *Biomacromolecules* 10(9):2686–2693. doi:[10.1021/bm900620w](https://doi.org/10.1021/bm900620w)
- Xiu ZM, Ma J, Alvarez PJJ (2011) Differential effect of common ligands and molecular oxygen on antimicrobial activity of silver nanoparticles versus silver ions. *Environ Sci Technol* 45(20):9003–9008. doi:[10.1021/es201918f](https://doi.org/10.1021/es201918f)
- Xiu Z, Zhang Q, Puppala HL, Colvin VL, Alvarez PJ (2012) Negligible particle-specific antibacterial activity of silver nanoparticles. *NanoLetters* 12(8):4271–4275
- Xu X, Brownlow W, Kyriacou S, Wan Q, Viola J (2004) Real-time probing of membrane transport in living microbial cells using single nanoparticle optics and living cell

- imaging. *Biochemistry* 43(32):10400–10413. doi:[10.1021/bi036231a](https://doi.org/10.1021/bi036231a)
- Zapata PA, Tamayo L, Páez M, Cerda E, Azócar I, Rabagliati FM (2011) Nanocomposites based on polyethylene and nanosilver particles produced by metallocenic “in situ” polymerization: synthesis, characterization, and antimicrobial behavior. *Eur Polym J* 47(8):1541. doi:[10.1016/j.eurpolymj.2011.05.008](https://doi.org/10.1016/j.eurpolymj.2011.05.008)
- Zhang Y-M, Rock CO (2008) Membrane lipid homeostasis in bacteria. *Nat Rev Microbiol* 6:222–233. doi:[10.1038/nrmicro1839](https://doi.org/10.1038/nrmicro1839)